

Electronic Coupling Effects on Photoinduced Electron Transfer in Carotene–Porphyrin–Fullerene Triads Detected by Time-Resolved EPR

Marilena Di Valentin,^{*,†} Arianna Bisol,[‡] Giancarlo Agostini,[‡] and Donatella Carbonera[‡]

Dipartimento di Scienze Chimiche, Università di Padova, via Marzolo 1, I-35131 Padova, Italy, and
CNR-Istituto di Chimica Biomolecolare, Sezione di Padova, via Marzolo 1, I-35131 Padova, Italy

Received May 3, 2005

Photoinduced charge separation and recombination in a carotenoid–porphyrin–fullerene triad C–P–C₆₀ (Bahr et al., 2000) have been followed by time-resolved electron paramagnetic resonance. The electron-transfer process has been characterized in a glass of 2-methyltetrahydrofuran and in the nematic phase of two uniaxial liquid crystals (E-7 and ZLI-1167). In all the different media, the molecular triad undergoes two-step photoinduced electron transfer, with the generation of a long-lived charge-separated state (C^{•+}–P–C₆₀^{•–}), and charge recombination to the triplet state, localized in the carotene moiety, mimicking different aspects of the photosynthetic electron-transfer process. The magnetic interaction parameters have been evaluated by simulation of the spin-polarized radical pair spectrum. The weak exchange interaction parameter ($J = +1.7 \pm 0.1$ G) provides a direct measure of the dominant electronic coupling matrix element V between the C^{•+}–P–C₆₀^{•–} radical pair state and the recombination triplet state ³C–P–C₆₀. Comparison of the estimated values of V for this triad and a structurally related triad differing only in the porphyrin bridge (octaalkylporphyrin vs tetraarylporphyrin) explains in terms of an electronic coupling effect the ~6-fold variation of the recombination rate induced by the modification of the porphyrin bridge as derived by kinetic experiments (Bahr et al., 2000).

1. INTRODUCTION

The design of organic molecules that mimic the photoinduced electron transfer (ET) process occurring in the natural photosynthetic reaction centers has traditionally involved porphyrins or chlorophyll derivatives, as chromophores and excited-state electron donors, that are covalently linked to electron acceptors such as quinones, other cyclic tetrapyrroles or organic molecules such as fullerenes, and to secondary donors such as carotenoid moieties.^{1–4}

In recent years, carotene (C)–porphyrin (P)–fullerene (C₆₀) molecular triads, differing one from the other in terms of small but significant structural changes, have been extensively investigated by both optical and magnetic time-resolved spectroscopies.^{5–12} These systems can be considered artificial photosynthetic reaction centers in their ability to mimic several key properties of the reaction center primary photochemistry.

Excitation of the porphyrin moiety of these molecules yields the first excited singlet state C–¹P–C₆₀, which undergoes photoinduced electron transfer to give C–P^{•+}–C₆₀^{•–} in a variety of polar solvents. Electron transfer from the carotenoid moiety competes with charge recombination, leading to the formation of a final C^{•+}–P–C₆₀^{•–} charge-separated state. This state is generated with high quantum yields. In most solvents, charge recombination of the secondary charge-separated state yields the carotenoid triplet state ³C–P–C₆₀, rather than the singlet ground state. Triplet

recombination of C^{•+}–P–C₆₀^{•–} is favored because the energy of the carotenoid triplet state is significantly below that of the secondary charge-separated state.¹³ The photochemistry of one of these triads (triad **1** in Chart 1) in 2-methyltetrahydrofuran (2-MeTHF) at room temperature is illustrated in Figure 1. The same photochemical behavior has been found also in the different phases of the liquid crystal (LC) solvents (E-7 and ZLI-1167).^{11,12}

In the C–P–C₆₀ molecular triads fine-tuning of the thermodynamic driving force and electronic coupling interactions has been achieved through structural modifications of the central porphyrin moiety, leading finally to optimal electron-transfer quantum yields ($\geq 96\%$). Replacement of the octaalkylporphyrin chromophore (triad **1**), with a tetraarylporphyrin (triad **2** in Chart 1), has produced the final result.¹⁰ Tetraarylporphyrins have higher oxidation potentials than the octaalkyl analogues, increasing therefore the thermodynamic driving force between the intermediate C–P^{•+}–C₆₀^{•–} and the final C^{•+}–P–C₆₀^{•–} charge-separated states.¹⁰ In addition, differences in frontier orbital densities^{10,14–16} and steric effects produced by the β -substituents^{17,18} are thought to lead to changes in electronic coupling between the porphyrin and the covalently attached donor and acceptor moieties.

A comparative investigation of molecular triads **1** and **2**, by time-resolved optical spectroscopies, revealed that tetraarylporphyrins, relative to alkyl-substituted porphyrins, reached the highest quantum yield of two-step charge separation because of the positive interplay between the rate of the charge shift reaction to produce the final C^{•+}–P–C₆₀^{•–} state from the intermediate C–P^{•+}–C₆₀^{•–} state (faster in triad **2**) and charge recombination of this state (slower in triad **2**),

* Corresponding author phone: +39-049-827-5139; fax: +39-049-827-5161; e-mail: marilena.divalentin@unipd.it.

[†] Università di Padova.

[‡] CNR-Istituto di Chimica Biomolecolare.

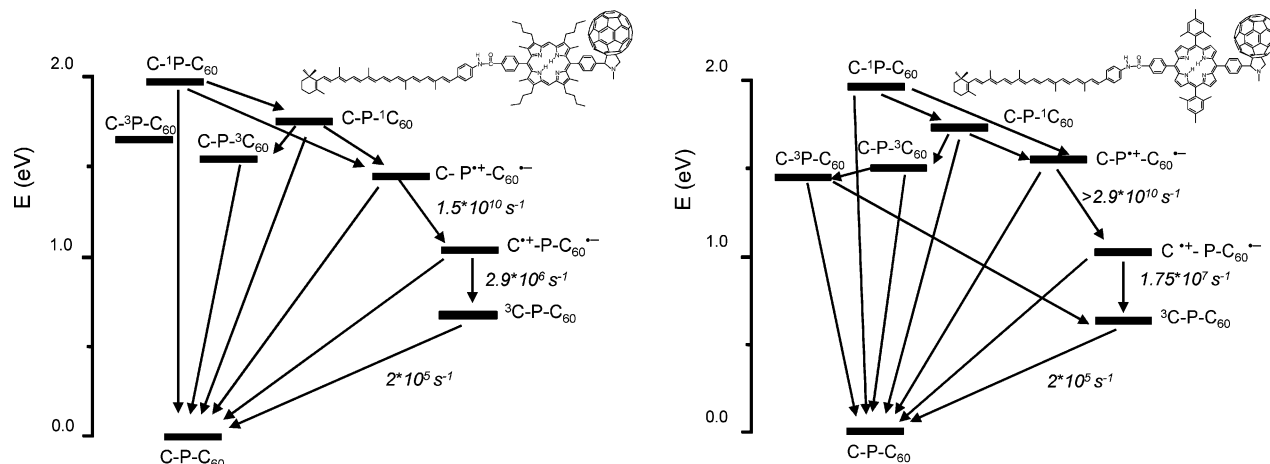
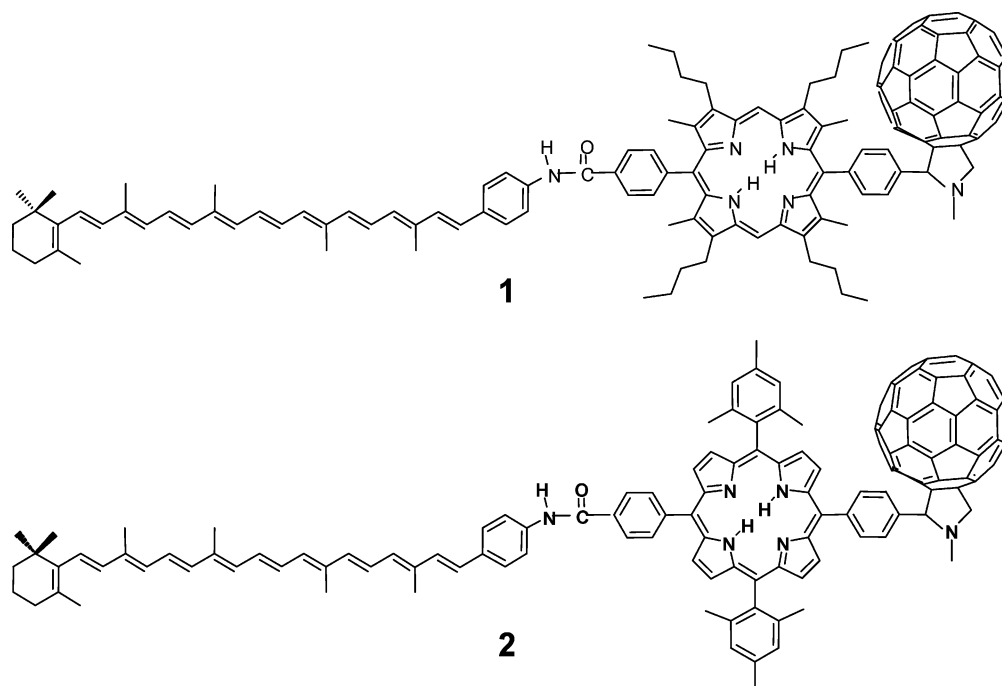


Figure 1. Relevant high energy states and interconversion pathways following excitation for triad **1** (left panel) and triad **2** (right panel). The energies of the various states have been estimated from spectroscopic and cyclic voltammetric data obtained in polar solvents.^{9,10}

Chart 1. Molecular Structures of Triad **1** and Triad **2**



induced by altering the structure of the porphyrin bridge.¹⁰

Time-resolved electron spin resonance (TREPR) spectroscopy is unique in revealing details relative to the ET process. Simulations of the spin-correlated radical pair spectrum allow to derive the exchange interaction parameter J , providing in this way a direct measure of the electronic coupling element V between the radical pair state and the electronic states that are energetically close to it.^{19–22} In the particular case of triad **1**, we have demonstrated that the exchange interaction between the carotene radical cation and the fullerene radical anion is related to only one dominant electronic coupling matrix element, the one connecting the $C^{+\bullet}-P-C_{60}^{\bullet-}$ radical pair state to the recombination triplet localized on the carotene moiety ${}^3C-P-C_{60}$.¹² The magnitude of the interaction ($J=0.5$ G) confirmed the role of the porphyrin bridge in mediating the electronic coupling between the carotene donor and the fullerene electron acceptor.^{6,11,12}

Improvement in the TREPR spectral analysis of the spin-correlated radical pair can be achieved using liquid crystal solvents. The anisotropy imposed by the nematic potential

on the guest molecules introduces orientational effects on the spectra, which provide additional information on the interaction parameters.²³ For example, the employment of LCs characterized by complementary alignment properties of the LC director with respect to the external magnetic field, and comparison of the effects produced on the TREPR spectra of the radical pair when going from a parallel to a perpendicular configuration, provide information on the relative contribution of the dipolar and exchange interaction parameters to the total magnetic spin–spin interaction.²⁴

The high degree of order achieved by molecular triad **1** in the LC and the detection of the spin-correlated radical pair in a wide temperature range allowed to fully exploit the convenient properties of LCs for TREPR investigation on the $C-P-C_{60}$ molecular triads.¹²

In the present study, the exchange interaction parameter J , corresponding to the $C^{+\bullet}-P-C_{60}^{\bullet-}$ radical pair state, is used to gain insight into the role of the porphyrin bridge in influencing the electron-transfer kinetics. For this reason the TREPR spectroscopy investigation, carried on molecular triad

1 in the glass of 2-methyltetrahydrofuran (2-MeTHF) and in the different phases of two uniaxial liquid crystals (E-7 and ZLI-1167), has been extended to molecular triad **2** in the same solvents. Evaluation of the exchange interaction parameter for triad **2** by spectral simulation of the $C^{\bullet+}-P-C_{60}^{\bullet-}$ spin-correlated radical pair and comparison with the corresponding value previously derived for triad **1**¹² provides direct evidence that modification of the porphyrin bridge directly affects the electronic coupling V between the carotenoid donor and the fullerene acceptor, proving the superexchange role played by the porphyrin bridge in the charge recombination kinetics.

2. MATERIALS AND METHODS

2.1. Materials. The synthesis of triad **2** has been reported elsewhere.¹⁰ The TREPR experiments were performed on the molecular triad either dissolved in purified 2-MeTHF (Sigma-Aldrich) or embedded and oriented in the liquid crystals E-7 and ZLI-1167 (Merck). E-7 is characterized by a positive diamagnetic susceptibility $\Delta\chi$ and a longitudinal dielectric constant $\epsilon_{||} = 19.6$, while ZLI-1167 has a negative $\Delta\chi$ and $\epsilon_{||} = 7.5$. The two LCs are characterized by the following phase transition temperatures:

E-7: crystalline \leftarrow 210 K \rightarrow soft glass \leftarrow 263 K \rightarrow nematic \leftarrow 333 K \rightarrow isotropic

ZLI-1167: crystalline \leftarrow 287 K \rightarrow smectic \leftarrow 305 K \rightarrow nematic \leftarrow 356 K \rightarrow isotropic

The LC samples ($\sim 1 \times 10^{-4}$ M) were prepared by dissolving triad **2** in toluene solution, evaporating the solvent to form a film of **2**, and then introducing E-7 or ZLI-1167. The 2-MeTHF samples ($\sim 1 \times 10^{-4}$ M) were prepared by dissolving **2** directly in the solvent. All the samples were deaerated by several freeze–thaw cycles and sealed under vacuum. TREPR experiments were performed on samples at different concentrations in order to rule out intermolecular processes or aggregation effects.

The alignment of the liquid crystal samples was carried out by exposing the nematic phase to an external high magnetic field (6000 G) for 10 min at ambient temperature and then cooling to the required temperature.²⁵ In the fluid nematic phase of E-7 the director **L** is aligned parallel to the external magnetic field **B**. In the case of the LC ZLI-1167, which features complementary properties, the mesophase director spans the plane perpendicular to **B**.

2.2. TREPR Measurements. Time-resolved EPR spectra were obtained in direct detection mode using pulsed light excitation. The X-band EPR spectrometer (Bruker ECS106) was equipped with a TE₁₀₂ cavity (9.4 GHz) and a nitrogen flow system. For measurements at cryogenic temperatures an Oxford helium cryostat (ESR 200) was used. Laser excitation at 532 nm (10 mJ per pulse and repetition rate of 10 Hz) was provided by the second harmonic of a Nd:YAG laser (Quantel Brilliant). Excitation at this wavelength yields mostly $C^{\bullet+}-P-C_{60}$. The time resolution of the TREPR spectrometer was ~ 200 ns. The microwave power used for the TREPR experiments was about 20 mW at the cavity. No field modulation or phase-sensitive detection was used. The EPR signals were taken from the microwave preamplifier (ER047-PH Bruker, bandwidth 20 Hz–6.5 MHz) and

sampled with a LeCroy LT364 oscilloscope (1 ns per point). To eliminate the laser background signal, transients were accumulated under off-resonance field conditions and subtracted from those on resonance. The spectra at different times after the laser pulse were reconstructed from kinetic traces for each field position.

2.3. TREPR Spectra Simulations. The radical pair spectral analysis was performed using programs written in MATLAB, based on the theoretical description of nondiffusing spin-correlated radical pairs as developed by P. Hore.²⁴

For each orientation of the molecule with respect to the external magnetic field **B**, without taking into account hyperfine interactions, which will be included in the inhomogeneous broadening, the spin-correlated radical pair spectrum consists of two doublets in antiphase of equal amplitude, centered at the Larmor frequencies of the individual radicals forming the pair. The splitting of each doublet is due to the exchange contribution J and the magnetic dipolar contribution D_{zz} . The frequencies of the four spin-polarized EPR lines are

$$\omega_{12} = \omega_0 - \Omega - J + D_{zz} \quad (1)$$

$$\omega_{34} = \omega_0 - \Omega + J - D_{zz}$$

$$\omega_{13} = \omega_0 + \Omega - J + D_{zz}$$

$$\omega_{24} = \omega_0 + \Omega + J - D_{zz}$$

where

$$\omega_0 = (\omega_A + \omega_B)/2$$

and ω_A and ω_B are the EPR frequencies of the two radicals in the absence of magnetic spin–spin interactions $\omega_A = g_A(\phi, \theta)\mu_B \hbar^{-1}B_0$ and $\omega_B = g_B(\phi, \theta)\mu_B \hbar^{-1}B_0$ where ϕ and θ denote the polar angles of the magnetic field **B** with respect to the axis system of the **g**-tensor,

$$D_{zz} = D(\cos^2\xi - 1/3)$$

being ξ the angle between the dipolar axis and the magnetic field direction **B**,

$$\Omega^2 = (J + D_{zz}/2)^2 + Q^2$$

and

$$Q = (\omega_A - \omega_B)/2$$

While the TREPR spectra in frozen solution reflect the powder average over all possible orientations, the partially ordered spectra in the LC medium have been calculated introducing a Gaussian orientational distribution function for the molecular alignment axis relative to the director of the mesophase **L**.²⁶ Assuming that the $C-P-C_{60}$ triad is an axially symmetric molecule, being characterized by a long molecular axis, the mean field orienting potential can be written as a function of only one angle, which describes the orientation of the molecular alignment axis with respect to **L**.

Simulations of the spin-polarized triplet spectra in 2-MeTHF were performed using a program written in FORTRAN,

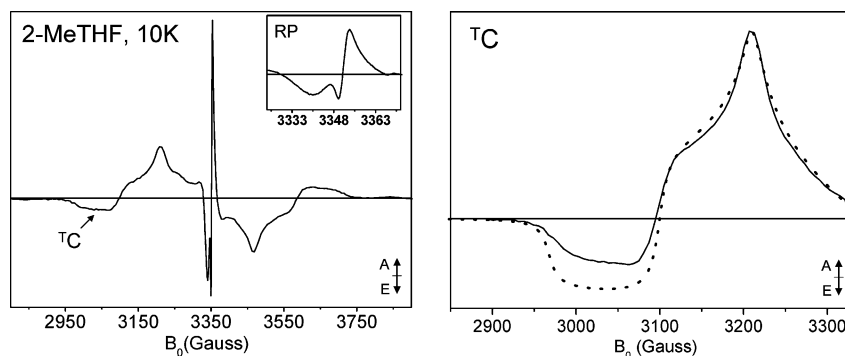


Figure 2. Left: TREPR spectrum of triad **2** in the isotropic glass of 2-Me-THF ($T=10$ K) at 250 ns after the laser pulse. The inset displays the expanded TREPR spectrum in the radical pair region. Right: TREPR semispectrum of $^3\text{C}-\text{P}-\text{C}_{60}$ (—) in the isotropic glass of 2-Me-THF ($T=10$ K) at 250 ns after the laser pulse and the corresponding powder triplet spectra simulations (---). The simulation parameters are reported in the text. A = absorption, E = emission.

assuming a powder distribution of molecular orientations and spin population differences reflecting the mechanism of recombination from a singlet born radical pair. The recombination triplet state can be identified by the unique polarization of the EPR transitions, that for a triplet state characterized by a negative value of the zero field splitting parameter D (rodlike molecules) is *eaeeea*. This polarization derives from $\text{S}-\text{T}_0$ mixing in the singlet-born weakly coupled radical pair and overpopulation of the T_0 triplet state at all canonical orientations due to the conservation of the spin angular momentum in the recombination process.²⁴

3. RESULTS

In our previous studies on molecular triad **1**, a complete characterization of the photophysical behavior of the molecule in the isotropic glass of 2-MeTHF¹¹ and in the different phases of the two LCs E-7 and ZLI-1167¹² has been performed, based on the spectral analysis of the TREPR signals corresponding to the paramagnetic species. In the LCs, the orientational dependence of the spectra, at different angles of the ordering director **L** relative to the external magnetic field **B**, has been analyzed in order to prove the high degree of order of the molecule inserted in LCs. Information on the mechanism of formation of the paramagnetic species in the LCs has been achieved, and the magnetic interaction parameters have been derived with more constraints, with respect to the isotropic solvent, and therefore allowing a better estimation of their values.

In the present study the same approach, in the main lines, is applied to molecular triad **2**, followed by comparison of the most significant results between the two triads differing in the structural and electronic characteristics of the porphyrin bridge joining the final donor and acceptor.

3.1. 2-Methyltetrahydrofuran Glass. The left panel of Figure 2 shows the spin-polarized EPR spectrum of triad **2** at 250 ns after the laser pulse in 2-MeTHF glass at 10 K. The EPR spectrum is similar in the main features to the one previously reported for triad **1** in the same experimental conditions,¹¹ although the relative intensity of the signals belonging to the photoexcited paramagnetic species is entirely different. In this case, the main contribution to the spectrum comes from the narrow radical pair signal (enlarged in the inset of Figure 2, left panel). Both antiphase doublets are present in the spectrum, one being only partially resolved.

Details and simulation of the radical pair signal, which has been attributed to the secondary charge-separated state $\text{C}^{+\bullet}-\text{P}-\text{C}_{60}^{\bullet-}$, will be shown in the next section.

The fulleropyrrolidine triplet, which was the main contribution to the spectrum of triad **1** in 2-MeTHF, has almost disappeared in the spectrum of triad **2**, a little contribution, spanning about 100 G, being still visible as positive and negative sidebands of the radical pair. The broad signal, characterized by the *eaeeea* polarization pattern, belongs to the carotenoid triplet (^1C in Figure 2). The assignment is based on the zero-field-splitting (ZFS) parameters²⁷ and comparison with previous experiments.

Although an *eaeeea* polarization pattern is compatible with a triplet recombination mechanism, the simulation of the powder triplet spectrum, shown in the right panel of Figure 2, does not fit perfectly the experimental spectrum, overestimating the contribution at the Z canonical orientation, associated with the largest component Z of the ZFS tensor. Simulations therefore prove that besides triplet recombination, which is certainly the dominant contribution to the spin polarization pattern observed, minor contributions, coming from a triplet state characterized by a somewhat different polarization pattern and therefore generated by a different mechanism, are present in the spectrum. Since there is no evidence of the presence of extra turning points in the triplet line shape which could be attributed to a triplet state characterized by different ZFS parameters, the only triplet state that has been detected is the carotenoid triplet states and in addition to the main route of recombination, triplet-triplet energy transfer from the porphyrin or fullerene triplet is likely contributing to the population of the carotenoid triplet.

3.2. Liquid Crystals E-7 and ZLI-1167. Figure 3 shows the spin-polarized EPR spectra of triad **2** at 250 ns from the laser flash in the nematic phase of E-7 at 295 K (left panel) and in the nematic phase of ZLI-1167 at 320 K (right panel). In both liquid crystals, featuring complementary orientational properties of the mesophase director with respect to the external magnetic field, the main contribution to the spectrum, as in 2-MeTHF glass, is the narrow $\text{C}^{+\bullet}-\text{P}-\text{C}_{60}^{\bullet-}$ radical pair signal at the center (enlarged in the insets of Figure 3). Both the antiphase doublets of the spin-correlated radical pair are distinguishable. The same *ea* polarization of the two doublets is observed for the $\text{L} \parallel \text{B}$ configuration of E-7 and for the $\text{L} \perp \text{B}$ configuration of ZLI-1167. In the

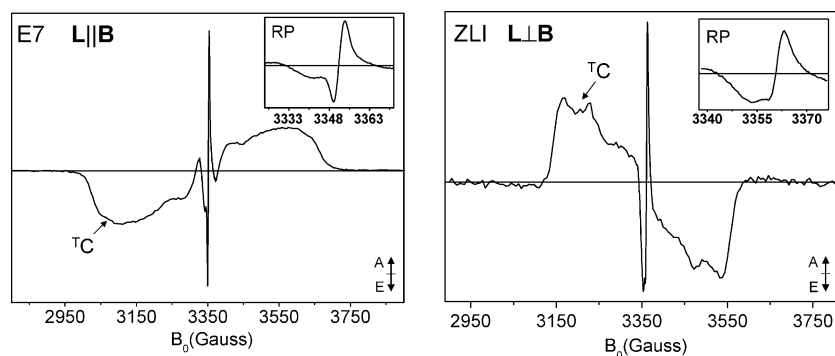


Figure 3. TREPR spectra of triad **2** at 250 ns after the laser pulse, in the liquid crystal nematic phase: (left panel) in E-7 ($T=296$ K) at the parallel configuration between the LC director and the external magnetic field ($\mathbf{L} \parallel \mathbf{B}$) and (right panel) in ZLI-1167 ($T=320$ K) at the perpendicular configuration ($\mathbf{L} \perp \mathbf{B}$). A = absorption, E = emission.

next section this result will be used to restrict the range of values of the magnetic interaction parameters.

Charge separation is achieved in high quantum yield throughout the overall range of the nematic phase in both LCs. The $\text{C}^{\bullet+}-\text{P}-\text{C}_{60}^{\bullet-}$ radical pair formation has been followed in all the different phases of the LC E-7 (data not shown); it occurs, with lower quantum yield, also in the crystalline phase and in the isotropic phase, up to a temperature of 345 K, where a spin-polarized radical pair signal is still detectable.

While the *N*-methylfulleropyrrolidine triplet contribution has almost disappeared, the broad spectral contribution spanning ~ 500 G comes from the carotenoid triplet $^3\text{C}-\text{P}-\text{C}_{60}$. Strong line shape effects have been produced by the nematic potential of the LC (pure emission contribution in E-7 and pure absorption in ZLI-1167), and the complete *eeaeaa* polarization of the powder spectrum in the isotropic glass of 2-MeTHF is lost. The partially ordered carotenoid triplet spectra in the $\mathbf{L} \parallel \mathbf{B}$ and $\mathbf{L} \perp \mathbf{B}$ configurations of the two LCs have been compared to the corresponding spectra obtained for triad **1** in the same experimental conditions.¹² A very similar orientation of the ZFS principal axes of the carotenoid triplet with respect to the director \mathbf{L} has been achieved for both molecular triads, as proved by the correspondence between spectra obtained in the same configuration \mathbf{L} vs \mathbf{B} . For triad **1**, a detailed analysis of the orientational dependence of the carotenoid triplet state has been performed, proving the high degree of order induced by the nematic potential in the direction of the long molecular axis.¹² The analogous orientational selection operated by the LCs on the carotenoid triplet spectra of triad **2** and the structural similarities between the two triads lead to the conclusion that a similar overall orientation is reached by the two molecules in both LCs, with the long molecular axis almost parallel to the LC director (see Figure 4).

In the LCs there is no evidence of the presence of a carotenoid triplet state with a spin polarization pattern arising from triplet–triplet energy transfer. Therefore the absence in the spectra of the fullerene triplet contribution could be due in this case to spin–lattice relaxation effects that, at the high temperatures reached in the nematic phase, could by themselves strongly affect the intensity of the fullerene triplet.

3.3. Spectral Analysis of the Spin-Correlated Radical Pair $\text{C}^{\bullet+}-\text{P}-\text{C}_{60}^{\bullet-}$. The orientational selection on the spectra of the triad **2** achieved in the LCs, as demonstrated in the last section, has been used to derive the magnetic interaction

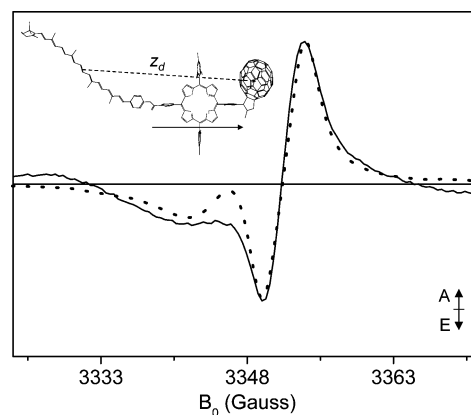


Figure 4. TREPR spectrum of the $\text{C}^{\bullet+}-\text{P}-\text{C}_{60}^{\bullet-}$ radical pair (—) at 250 ns after the laser pulse in the nematic phase of E-7 ($T=296$ K) and best-fit spectral simulation (---). The simulation parameters are reported in Table 1. A = absorption, E = emission. In the molecular structure, the long axis direction and the dipolar vector z_d of $\text{C}^{\bullet+}-\text{P}-\text{C}_{60}^{\bullet-}$ are shown.

parameters and discuss them in terms of comparison with those obtained in the previous analysis on triad **1**.¹² In Figure 4 the calculated TREPR spectrum of the partially ordered spin-correlated radical pair has been superimposed to the spin-polarized experimental spectrum at 250 ns from the laser flash in the nematic phase of E-7 (295 K). All the simulation parameters, discussed in the next paragraphs, are reported in Table 1.

The spectral analysis has been performed in the correlated radical pair mechanism (CRPM) framework,²⁴ described in the Materials and Methods section, which has been extended to partially ordered samples by introducing a Gaussian orientational distribution function for the molecular alignment axis relative to the director of the mesophase. The same distribution function, estimated from the detailed analysis of the oriented carotenoid triplet spectra performed for triad **1** and used in the simulation of the spin-correlated radical pair spectrum, has been applied to triad **2**, given the similarities found in the orientational selection between the two molecules. In this way, it was possible to avoid the introduction of extra variable parameters in this comparative analysis. No important variation of the distribution function should be expected for the two triads, which are structurally very similar.

No evolution of the spin polarization due to kinetic or relaxation effects has been considered, and for this reason the initial spin-polarized experimental spectrum has been

Table 1. Spectral Parameters Used for the $C^{\bullet+}$ -P- $C_{60}^{\bullet-}$ Radical Pair Spectrum Simulation Reported in Figure 4 According to the SCRP Model²⁴

g -tensors ^a	g_{xx}	g_{yy}	g_{zz}	$\langle g \rangle^b$
$C^{\bullet+}$	2.00335	2.00251	2.00227	2.00271
$C_{60}^{\bullet-}$				2.00023
spin-spin coupling of $C^{\bullet+}PC_{60}^{\bullet-}$				
	D		-0.6 G	
	J		+1.7 ± 0.1 G	
tensor orientations ^c		α	β	γ
g -tensor of $C^{\bullet+}$		90°	90°	30°
D -tensor of $C^{\bullet+}PC_{60}^{\bullet-}$		0°	0°	
$\Delta H_{1/2}^d$				
$C^{\bullet+}$			12 G	
$C_{60}^{\bullet-}$			7 G	

^a Estimated error: ±0.0005. ^b The isotropic g -value. ^c The tensor orientation expressed in terms of Euler angles are given for rotation about Z by α , Y' by β , and Z' by γ , in the fixed molecular frame with the Z direction along the long molecular axis. Estimated error: ±5°. ^d $\Delta H_{1/2}$ is the full line width at half-height. Uncertainty: ±5%.

compared to the calculated spectrum. Furthermore, agreement between simulation and the initial experimental spectrum has been obtained assuming that the radical pair is generated from a singlet precursor and the spin polarization arises in the secondary $C^{\bullet+}$ -P- $C_{60}^{\bullet-}$ radical pair meaning that the lifetime of C -P $^{\bullet+}$ - $C_{60}^{\bullet-}$ is maintained very short also in the LC nematic phase.

The best-fit parameter of the simulations is the exchange interaction parameter J , while the dipolar coupling between the two spins, described by a zero-field tensor with axial symmetry, is introduced as a fixed parameter and has been estimated in the point-dipole approximation given the large center-to-center distance between the two radicals. The same average center-to-center distance of ~36 Å has been found for both triad **1** and **2**, corresponding to the minimum-energy structures obtained from molecular modeling calculations (ChemBats3D/MM2) and therefore the dipolar parameter being the same ($D = -0.6$ G) for the two triads. For the simulations, the dipolar axis (z_d) is taken to be roughly parallel to the long axis of the molecule, as shown in Figure 4, and it is therefore aligned with the LC director **L**.

The radical magnetic parameters, g -tensors, and inhomogeneous line widths are also introduced as fixed parameters in the simulations. These parameters come from X-band and high field CW-EPR experiments on β -carotene and N -methylfulleropyrrolidine radicals,^{28–33} and their values and tensor orientations have already been adjusted for the best-fit of $C^{\bullet+}$ -P- $C_{60}^{\bullet-}$ radical pair spectra, performed on triad **1**.¹² All the parameters, except for the exchange parameter J , are kept the same in the simulations of the radical pair of **1** and **2**, to avoid introducing extra variables and focus the comparative analysis on the exchange interaction. No significant variation of the magnetic parameters of the two radicals is expected since the structural variation does not affect them directly. The error margins on the spectral parameters, reported in Table 1, affect the output value for the parameter J within the confidence interval of ±0.1 G.

The best value for the exchange interaction parameter J is +1.7 ± 0.1 G. The same value for J can satisfactory

reproduce the features of the powder radical-pair spectrum in 2-MeTHF glass and of the partially ordered spectrum in the **L** ⊥ **B** configuration of ZLI-1167.

Again, as in the case of triad **1**, the exchange interaction makes a substantial contribution to the total spin-spin coupling, despite the large center-to-center separation between the carotene and fullerene radicals. The only disagreement with the experimental results is that the broader antiphase doublet attributed to the carotenoid radical is underestimated in the calculated spectrum. Dynamic effects such as different relaxation rates for the two radicals could be responsible for this effect. In the isotropic phase at high temperature (data not shown), the carotenoid contribution becomes even more pronounced, confirming therefore this hypothesis.

Only the interplay between the negative value of the dipolar parameter D , as derived in the point-dipole approximation, and a positive value of the J parameter results in the ea polarization of the two antiphase doublets. Zero or negative values of the exchange parameter produce an opposite ae pattern and can be therefore excluded. Furthermore, the absence of phase inversion of the radical pair spectrum, when going from the **L** || **B** configuration (in E-7) to the **L** ⊥ **B** configuration (in ZLI-1167), is an important indication, according to the correlated radical pair sign rule,²⁴ that the exchange interaction must contribute significantly together with the dipolar interaction to the splitting of the spin-correlated radical pair doublets, despite the large distance between the donor and acceptor moieties.

4. DISCUSSION

The approach used in this work is to derive the magnetic exchange interaction parameter relative to the radical pair state $C^{\bullet+}$ -P- $C_{60}^{\bullet-}$ from line shape analysis of the TREPR spectrum of the spin-correlated radical pair and use the value obtained for J to evaluate the electronic coupling matrix element V of the ET reaction between this state and the electronic states that are energetically close to it. Experimental evaluation of the exchange parameter J provides important insight into the effects on electronic coupling induced by small structural changes of the radical pair and therefore provides important information on how to optimize the molecular structure in order to improve the photochemistry of the triad under investigation.

The electron transfer behavior of triad **2** has been fully characterized in 2-MeTHF at ambient temperature by optical time-resolved spectroscopy.¹⁰ The TREPR experiments have been performed in the glass phase of 2-MeTHF at 10 K, to reduce the effects of spin relaxation which preclude detection of a spin-polarized radical pair at high temperatures. As expected, in analogy to the behavior of the other C-P- C_{60} molecular triads,^{9,11} charge separation occurs also in the glass of 2-MeTHF because of the lack of sensitivity of the fullerene anion to solvent effects.^{9,34,35} The TREPR investigation has been extended to two different LCs, E-7 and ZLI-1167, which feature complementary properties in terms of orientation of the director with respect to the static magnetic field. Triad **2** has been successfully inserted in the LCs, where a high degree of order has been achieved. Furthermore, in the nematic phase of both solvents, charge separation occurs in high quantum yields.

It is necessary to use LCs in order to get as much information as possible from the spectral analysis of the spin-correlated radical pair. The orientational effects introduced in the spectra by the anisotropy induced by the nematic potential on the orientation of the triads has been used to restrict the range of plausible values for the exchange parameter J . This becomes particularly important if we want to relate this parameter to the electronic coupling matrix element V and discuss it in terms of the effects induced in the ET kinetics.

Although the main aim of this investigation was to determine the electronic coupling matrix element V for the electron-transfer reaction, relevant information on the photochemistry of this triad has been derived from the initial spin polarization of the TREPR signals, which is indicative of the mechanism of formation of the paramagnetic species. Line shape analysis of an initial TREPR spectrum of the carotenoid triplet state in 2-MeTHF glass at 10 K has shown that the polarization pattern cannot be reproduced assuming exclusive population of the T_0 spin sublevel, as expected for the charge recombination mechanism from a singlet radical pair.²⁴ The lack of extra spectral features that would be introduced by the contribution of a different triplet state to the spectrum demonstrate that in addition to charge recombination, a small fraction of the carotenoid triplet state is populated by triplet–triplet energy transfer.

Transfer of triplet excitation from the fullerene moiety to the carotenoid was already demonstrated for triad **1** and was effective in toluene at ambient temperature and in 2-MeTHF down to about 150 K.⁸ The temperature dependence of the triplet energy transfer was investigated in 2-MeTHF in order to distinguish between a single-step and a two-step energy transfer. A two-step relay mechanism, involving a slow endergonic transfer from the fullerene triplet $C-P-^3C_{60}$, populated by intersystem crossing, to the porphyrin triplet $C-^3P-C_{60}$, followed by rapid exergonic transfer to the final carotenoid triplet state $^3C-P-C_{60}$, was demonstrated (see Figure 1). Triplet–triplet energy transfer has completely ceased at 77 K, in agreement with the presence of the fullerene triplet signal in the TR-EPR spectrum on triad **1** in 2-MeTHF at 10 K.¹¹ For triad **1**, the fullerene triplet, whose polarization derives from a mechanism of intersystem crossing,³⁶ is the most important contribution in terms of intensity to the EPR spectrum in the glass at 10 K, and the spin polarization of the carotenoid triplet is consistent with a mechanism of charge recombination from a singlet radical pair.

Structural modification of the porphyrin bridge, when going from triad **1** to triad **2**, produced a variation of the porphyrin triplet energy. While the triplet state of octaalkylporphyrins is located at 1.61 eV, higher in energy than the fullerene triplet state, the triplet state of the tetraarylporphyrin is located at 1.45 eV, below the fullerene triplet (see Figure 1).³⁷ This would explain the strongly reduced intensity of the fullerene triplet in the TREPR spectrum of triad **2** in 2-MeTHF glass at 10 K and the unsatisfactory simulation of the carotenoid recombination triplet shown in the right panel of Figure 2. In the case of triad **2**, the two-step energy transfer process can occur down to cryogenic temperatures since the structural modifications introduced in this triad have produced a completely exergonic pathway. The fullerene triplet, populated as side product of the photoexcitation

process by intersystem crossing, rapidly disappears, and triplet energy is then efficiently transferred to the carotenoid through the porphyrin triplet. The main mechanism of formation of the carotenoid triplet remains however charge recombination from the $C^+-P-C_{60}^{\bullet-}$ radical pair state.

In the LCs E-7 and ZLI-1167 the absence of the fullerene triplet signal, as already mentioned in the previous section, cannot be used as evidence of triplet–triplet transfer to the carotenoid triplet and spin–lattice relaxation effects, at the high temperatures reached in the nematic phase of the LCs, can be responsible for the lack of a significant fullerene triplet contribution to the spectra. What is a clear experimental evidence is, however, the fact that charge separation and triplet charge recombination to the carotenoid triplet is effective also in the nematic phase of both E-7 and ZLI-1167 LCs.

Once the photochemistry of triad **2** has been fully characterized, the magnetic interaction parameters of the $C^+-P-C_{60}^{\bullet-}$ radical pair state can be discussed and compared to those corresponding to triad **1**.¹²

Simulations of the $C^+-P-C_{60}^{\bullet-}$ radical pair have confirmed the spin-correlated nature of the radical pair and allowed identification of the partners of the charge-separated state, the carotenoid radical cation, and the *N*-methylfullepyrrolidine radical anion. An exchange interaction parameter J value of $+1.7 \pm 0.1$ G has been evaluated from the simulation of the spectrum in E-7 while the ZFS parameter $D = -0.6$ G has been calculated in the point-dipole approximation, as in our previous work on triad **1**.¹² The non zero-value found for the exchange parameter is supported by the experimental observation that no effect on the spin polarization of the spectrum is produced when going from the $L \parallel B$ configuration of E-7 to the $L \perp B$ configuration of ZLI-1167, as expected only when the exchange interaction makes a substantial contribution to the splitting of the EPR doublets.

The exchange interaction parameter has been used thereafter to evaluate the electronic coupling matrix element V of the ET between the charge separated state $C^+-P-C_{60}^{\bullet-}$ and the electronic states that are energetically close. The singlet–triplet splitting within the radical pair ($2J$) is a sum of the squares of the electronic coupling elements of the charge separated state with the ground state and the excited states, weighted on the energy splitting between the radical pair state and these states:^{19,20,22}

$$2J = E_S - E_T = \left[\sum_n \frac{V_n^2}{\Delta E_{nS}} \right] - \left[\sum_n \frac{V_n^2}{\Delta E_{nT}} \right] \quad (2)$$

where ΔE_n is the vertical energy separation between the radical pair state and the interacting state at the equilibrium nuclear configuration of $C^+-P-C_{60}^{\bullet-}$. The individual terms, in both the singlet and triplet manifolds in eq 2, may be ferromagnetic or antiferromagnetic depending on the sign of the corresponding energy term.

On the basis of the energy splitting terms at the denominator, the dominant contribution should be the electronic coupling of the $C^+-P-C_{60}^{\bullet-}$ triplet radical pair state with the recombination triplet state $^3C-P-C_{60}$, as already demonstrated for triad **1**.¹² A single-term expression for J is therefore obtained:

$$2J = -\frac{V_{\text{CRT}}^2}{\Delta E_{\text{CRT}}} = -\frac{V_{\text{CRT}}^2}{\Delta G_{\text{CRT}}^0 + \lambda} \quad (3)$$

The energy splitting term can be calculated by adding the free energy difference for the reaction ΔG° and the total reorganization energy λ . ΔE_{CRT} was estimated using the electrochemical data for the free energy $\Delta G^\circ = 0.4 \text{ eV}^{10}$ and a value for the reorganization energy $\lambda = 0.5 \text{ eV}$, which was previously used to derive the electronic coupling matrix element in the case of triad **1** and which is compatible with the low reorganization energy reported for the fullerene-based systems.^{38,39}

The matrix element relative to triplet charge recombination V_{CTR} can then be evaluated from the exchange interaction parameter J , determined from the radical pair spectra. The value obtained for V_{CTR} using eq 3 is 0.5 cm^{-1} .

Once the electronic coupling has been estimated, comparison can be made between the charge recombination rates of the two triads. The semiclassical Marcus-Jortner theory of electron transfer predicts that the ET rate is directly proportional to V^2 .⁴⁰

$$k_{\text{ET}} = \frac{2\pi}{\hbar} V^2 \frac{1}{\sqrt{4\pi\lambda k_{\text{B}}T}} \exp\left[-\frac{(\Delta G^\circ + \lambda)^2}{4\lambda k_{\text{B}}T}\right] \quad (4)$$

A ~ 6 -fold difference in recombination rates between **1** and **2** has been measured by time-resolved optical spectroscopy in 2-MeTHF at room temperature (values reported in Figure 1).¹⁰ Being the $\text{C}^+-\text{P}-\text{C}_{60}^{\bullet-}$ states in **1** and **2** essentially isoenergetic, as the carotenoid and the fullerene moieties can be considered identical in the two triads, the driving force for charge recombination to the triplet state is identical for the two molecules. For this reason the ~ 6 -fold difference in recombination rates was tentatively attributed to pure electronic coupling factors. Direct comparison of the electronic coupling matrix elements V^2 , derived from the exchange interaction parameter and therefore from TREPR experiments ($V = 0.27 \text{ cm}^{-1}$ for triad **1**¹² and $V = 0.5 \text{ cm}^{-1}$ for triad **2**), gives an ~ 3 -fold difference in recombination rates, assuming all the other factors to be unchanged. A small difference in driving force or in reorganization energy cannot however be completely excluded. An ~ 3 -fold difference is a good estimation, in view of the crude approximations adopted for the calculation.

The result is certainly important since the TREPR spectroscopy has shown to be able to provide a direct and highly sensitive method to determine the electronic coupling matrix elements. The experimental observation of faster recombination in **2** with respect to **1** has found its counterpart in the experimental determination of V through the magnetic exchange interaction parameter J , proving in this way that the exchange interaction parameter J has been properly estimated in this and related triads.^{6,11,12} Furthermore, a substantial increase of electronic coupling when going from triad **1** to triad **2** where only the porphyrin bridge has been structurally modified, in agreement with the experimentally measured effect on charge recombination rates, is conclusive evidence of the involvement of the porphyrin π -electron system in the electronic coupling between the carotenoid donor and the fullerene acceptor, which was previously proposed considering only the distance dependence of V .^{6,11,12}

Increased electronic coupling when going from the octaalkyl to the tetraarylporphyrin bridge finds theoretical explanation, as previously suggested, in considering both steric and frontier orbital density distribution effects.^{14–18} In octaalkyl porphyrins, through steric effects, the β -substituents of the porphyrin moiety inhibit rotation of the adjacent aryl rings, forcing them in a more orthogonal conformation,¹⁸ with the consequence of reducing the electronic coupling between the porphyrin and the fullerene moieties, which involves the linkage bonds and therefore the π -system of the aryl rings.¹⁷ The steric arguments are supported by considerations on the nature of the frontier molecular orbitals; porphyrin with β -substituents have a_{1u} highest occupied molecular orbitals (HOMOs), while the tetraarylporphyrins have a_{2u} -type HOMOs. The a_{1u} HOMO has nodes at the *meso* positions, while the a_{2u} HOMO has lobes at the same positions, reducing in the first case the electronic coupling between the porphyrin and the fullerene and enhancing it in the second case.^{14–16} Both the steric effects and orbital ordering favor therefore electronic coupling in tetraaryl-based triads, in agreement with both optical spectroscopy¹⁰ and TREPR results.

As a concluding remark, TREPR provides a spectroscopic tool for the direct measure of the dominant electronic coupling matrix element V between the $\text{C}^+-\text{P}-\text{C}_{60}^{\bullet-}$ radical pair state and the recombination triplet state $^3\text{C}-\text{P}-\text{C}_{60}$. Comparison of the estimated values of V for triad **2** and a structurally related triad differing only in the porphyrin bridge (octaalkylporphyrin vs tetraarylporphyrin) explains in terms of a pure electronic coupling effect the ~ 6 -fold variation of the recombination rate induced by the modification of the porphyrin bridge as derived by kinetic experiments,¹⁰ which finds, as already suggested, theoretical explanation in the differences in steric effects and frontier orbital densities between the two porphyrin bridges.

ACKNOWLEDGMENT

This work was supported by the PRIN project no. 2002031443, by the CNR project no. CNRG004079. The authors are indebted to Paul A. Liddell, Ana L. Moore, Thomas A. Moore, and Devens Gust for synthesizing and providing the carotene–porphyrin–fullerene molecular triad and for stimulating discussions about the photophysics of the model systems. The authors thank Dr. Michael Fuhs for providing the simulation program for the spin-correlated radical pair spectra.

REFERENCES AND NOTES

- (1) Wasielewski, M. R. Photoinduced Electron Transfer in Supramolecular Systems for Artificial Photosynthesis. *Chem. Rev.* **1992**, 92, 435–461.
- (2) Kurreck, H.; Huber, M. Model Reactions for Photosynthesis-Photoinduced Charge and Energy Transfer between Covalently Linked Porphyrin and Quinone Units. *Angew. Chem., Int. Ed. Engl.* **1995**, 34, 849–866.
- (3) Gust, D.; Moore, T. A.; Moore, A. L. Mimicking Bacterial Photosynthesis. *Pure Appl. Chem.* **1998**, 70, 2189–2200.
- (4) Moore, T. A.; Moore, A. L.; Gust, D. The Design and Synthesis of Artificial Photosynthetic Antennas, Reaction Centers and Membranes. *Philos. Trans. R. Soc. London, Ser. B* **2002**, 357, 1481–1498.
- (5) Liddell, P. A.; Kuciauskas, D.; Sumida, J. P.; Nash, B.; Nguyen, D.; Moore, A. L.; Moore, T. A.; Gust, D. Photoinduced Charge Separation and Charge Recombination to a Triplet State in a Carotene-Porphyrin-Fullerene Triad. *J. Am. Chem. Soc.* **1997**, 119, 1400–1405.
- (6) Carbonera, D.; Di Valentin, M.; Corvaja, C.; Agostini, G.; Giacometti, G.; Liddell, P. A.; Kuciauskas, D.; Moore, A. L.; Moore, T. A.; Gust, D. EPR Investigation of Photoinduced Radical Pair Formation and

- Decay to a Triplet State in a Carotene-Porphyrin-Fullerene Triad. *J. Am. Chem. Soc.* **1998**, *120*, 4398–4405.
- (7) Kuciauskas, D.; Liddell, P. A.; Moore, A. L.; Moore, T. A.; Gust, D. Magnetic Switching of Charge Separation Lifetimes in Artificial Photosynthetic Reaction Centers. *J. Am. Chem. Soc.* **1998**, *120*, 10880–10886.
 - (8) Gust, D.; Moore, T. A.; Moore, A. L.; Kuciauskas, D.; Liddell, P. A.; Halbert, B. D. Mimicry of Carotenoid Photoprotection in Artificial Photosynthetic Reaction Centers: Triplet–Triplet Energy Transfer by a Relay Mechanism. *J. Photochem. Photobiol. B* **1998**, *43*, 209–216.
 - (9) Kuciauskas, D.; Liddell, P. A.; Lin, S.; Stone, S. G.; Moore, A. L.; Moore, T. A.; Gust, D. Photoinduced Electron Transfer in Carotenoporphyrin-Fullerene Triads: Temperature and Solvent Effects. *J. Phys. Chem. B* **2000**, *104*, 4307–4321.
 - (10) Bahr, J. L.; Kuciauskas, D.; Liddell, P. A.; Moore, A. L.; Moore, T. A.; Gust, D. Driving Force and Electronic Coupling Effects on Photoinduced Electron Transfer in a Fullerene-based Molecular Triad. *Photochem. Photobiol.* **2000**, *72*, 598–611.
 - (11) Di Valentin, M.; Bisol, A.; Giacometti, G.; Carbonera, D.; Agostini, G.; Liddell, P. A.; Moore, A. L.; Moore, T. A.; Gust, D. Reaction Center Models in Liquid Crystals: Identification of Paramagnetic Intermediates. *Mol. Cryst. Liq. Cryst.* **2003**, *394*, 19–30.
 - (12) Di Valentin, M.; Bisol, A.; Agostini, G.; Fuhs, M.; Liddell, P. A.; Moore, A. L.; Moore, T. A.; Gust, D.; Carbonera, D. Photochemistry of Artificial Photosynthetic Reaction Centers in Liquid Crystals Probed by Multifrequency EPR (9.5 and 95 GHz). *J. Am. Chem. Soc.* **2004**, *126*, 17074–17086.
 - (13) Lewis, J. E.; Moore, T. A.; Benin, D.; Gust, D.; Nicodem, D.; Nonell, S. *Photochem. Photobiol.* **1994**, *59S*, 35.
 - (14) Strachan, J. P.; Gentemann, S.; Seth, J.; Kalsbeck, W. A.; Lindsey, J. S.; Holten, D.; Bocian, D. F. Effects of Orbital Ordering on Electronic Communication in Multiporphyrin Arrays. *J. Am. Chem. Soc.* **1997**, *119*, 11191–11201.
 - (15) Yang, S. I.; Seth, J.; Balasubramanian, T.; Kim, D.; Lindsey, J. S.; Holten, D.; Bocian, D. F. Interplay of Orbital Tuning and Linker Location in Controlling Electronic Communication in Porphyrin Arrays. *J. Am. Chem. Soc.* **1999**, *121*, 4008–4018.
 - (16) Kuciauskas, D.; Liddell, P. A.; Lin, S.; Johnson, T. E.; Weghorn, S. J.; Lindsey, J. S.; Moore, A. L.; Moore, T. A.; Gust, D. An Artificial Photosynthetic Antenna-Reaction Center Complex. *J. Am. Chem. Soc.* **1999**, *121*, 8604–8614.
 - (17) Kuciauskas, D.; Liddell, P. A.; Hung, S. C.; Stone, S. G.; Seely, G. R.; Moore, A. L.; Moore, T. A.; Gust, D. Structural Effects on Photoinduced Electron Transfer in Carotenoid-Porphyrin-Quinone Triads. *J. Phys. Chem. B* **1997**, *101*, 429–440.
 - (18) Noss, L.; Liddell, P. A.; Moore, A. L.; Moore, T. A.; Gust, D. Aryl Ring Rotation in Porphyrins. A Carbon-13 NMR Spin–lattice Relaxation Time Study. *J. Phys. Chem. B* **1997**, *101*, 458–465.
 - (19) Anderson, P. W. New Approach to the Theory of Superexchange Interactions. *Phys. Rev.* **1959**, *115*, 2–13.
 - (20) Volk, M.; Häberle, T.; Feick, R.; Ogorodnik, A.; Michel-Beyerle, M. E. What can be learned from the Singlet–Triplet Splitting of the Radical Pair P^+H^- in the Photosynthetic Reaction Center? Conclusions from Electric Field Effects on the P^+H^- Recombination Dynamics. *J. Phys. Chem.* **1993**, *97*, 9831–9836.
 - (21) Calvo, R.; Abresch, E. C.; Bittl, R.; Feher, G.; Hofbauer, W.; Isaacson, R. A.; Lubitz, W.; Okamura, M. Y.; Paddock, M. L. EPR Study of the Molecular and Electronic Structure of the Semiquinone Biradical $Q_A^{\bullet-}Q_B^{\bullet-}$ in Photosynthetic Reaction Centers from Rhodospirillum rubrum. *J. Am. Chem. Soc.* **2000**, *122*, 7327–7341.
 - (22) Weiss, E. A.; Ratner, M. A.; Wasielewski, M. R. Direct Measurement of Singlet–Triplet Splitting within Rodlike Photogenerated Radical Ion Pairs using Magnetic Field Effects: Estimation of the Electronic Coupling for Charge Recombination. *J. Phys. Chem. A* **2003**, *107*, 3639–3647.
 - (23) Levanon, H.; Möbius, K. Advanced EPR Spectroscopy on Electron-Transfer Processes in Photosynthesis and Biomimetic Model Systems. *Annu. Rev. Biophys. Biomol. Struct.* **1997**, *26*, 495–540.
 - (24) Hore, P. J. In *Advanced EPR*; Hoff, A. J., Ed.; Elsevier Science Publishers B.V.: Amsterdam, 1989; Chapter 12, pp 405–440.
 - (25) Gonen, O.; Levanon, H. Time-resolved EPR Spectroscopy of Electron Spin Polarized ZnTPP Triplets oriented in a Liquid Crystal. *J. Phys. Chem.* **1985**, *89*, 1637–1643.
 - (26) Fuhs, M.; Elger, G.; Osintsev, A.; Popov, A.; Kurreck, H.; Möbius, K. Multifrequency Time-resolved EPR (9.5 GHz and 95 GHz) on Covalently Linked Porphyrin-Quinone Model Systems for Photosynthetic Electron Transfer: Effect of Molecular Dynamics on Electron Spin Polarization. *Mol. Phys.* **2000**, *98*, 1025–1040.
 - (27) Carbonera, D.; Di Valentin, M.; Agostini, G.; Giacometti, G.; Liddell, P. A.; Gust, D.; Moore, A. L.; Moore, T. A. Energy Transfer and Spin Polarization of the Carotenoid Triplet State in Synthetic Carotenoporphyrin Dyads and in Natural Antenna Complexes. *Appl. Magn. Reson.* **1997**, *13*, 487–504.
 - (28) Lakshmi, K. V.; Reifler, M. J.; Brudvig, G. W.; Poluektov, O. G.; Wagner, A. M.; Thurnauer, M. C. High-field EPR Study of Carotenoid and Chlorophyll Cation Radicals in Photosystem II. *J. Phys. Chem. B* **2000**, *104*, 10445–10448.
 - (29) Faller, P.; Rutherford, A. W.; Un, S. High-Field EPR Study of Carotenoid $^{+}$ and the Angular Orientation of Chlorophyll z^{+} in Photosystem II. *J. Phys. Chem. B* **2000**, *104*, 10960–10963.
 - (30) Grant, J. L.; Kramer, V. J.; Ding, R.; Kispert, L. D. Carotenoid Cation Radicals: Electrochemical, Optical, and EPR Study. *J. Am. Chem. Soc.* **1988**, *110*, 2151–2157.
 - (31) Sun, Y.; Drovetskaya, T.; Bolskar, R. D.; Bau, R.; Boyd, P. D. W.; Reed, C. A. Fullerides of Pyrrolidine-functionalized C_{60} . *J. Org. Chem.* **1997**, *62*, 3642–3649.
 - (32) Zoleo, A.; Maniero, A. L.; Prato, M.; Severin, M. G.; Brunel, L. C.; Kordatos, K.; Brustolon, M. Anion Radicals of Mono- and Bisfulleropyrrolidines: g Tensors, Spin Density Distribution and Spin–Lattice Relaxation. *J. Phys. Chem. A* **2000**, *104*, 9853–9863.
 - (33) Brustolon, M.; Zoleo, A.; Agostini, G.; Maggini, M. Radical Anions of Mono- and Bis-fulleropyrrolidines: an EPR Study. *J. Phys. Chem. A* **1998**, *102*, 6331–6339.
 - (34) Guldi, D. M.; Luo, C.; Da Ros, T.; Bosi, S.; Prato, M. Small Reorganization Energy and Unique Stabilization of Zwitterionic C_{60} -Acceptor Moieties. *Chem. Commun.* **2002**, *20*, 2320–2321.
 - (35) Guldi, D. M.; Luo, C.; Kotov, N. A.; Da Ros, T.; Bosi, S.; Prato, M. Zwitterionic Acceptor Moieties: Small Reorganization Energy and Unique Stabilization of Charge-Transfer Products. *J. Phys. Chem. B* **2003**, *107*, 7293–7298.
 - (36) Pasimeni, L.; Segre, U.; Ruzzi, M.; Maggini, M.; Prato, M.; Kordatos, K. Preferential Orientation of Fulleropyrrolidine Bisadducts in E7 Liquid Crystal: a Time-resolved Electron Paramagnetic Resonance Study. *J. Phys. Chem. B* **1999**, *103*, 11275–11281.
 - (37) Gouterman, M.; Khalil, G.-E. Porphyrin Free Base Phosphorescence. *J. Mol. Spectrosc.* **1974**, *53*, 88–100.
 - (38) Guldi, D. M. Fullerene-Porphyrin Architectures; Photosynthetic Antenna and Reaction Center Models. *Chem. Soc. Rev.* **2002**, *31*, 22–36.
 - (39) Imahori, H.; Yamada, H.; Guldi, D. M.; Endo, Y.; Shimomura, A.; Kundu, S.; Yamada, K.; Okada, T.; Sakata, Y.; Fukuzumi, S. Comparison of Reorganization Energies for Intra- and Intermolecular Electron Transfer. *Angew. Chem., Int. Ed.* **2002**, *41*, 2344–2347.
 - (40) Marcus, R. A.; Sutin, N. Electron transfers in Chemistry and Biology. *Biochim. Biophys. Acta* **1985**, *811*, 265–322.

CI050183E